

GPS-SSL: GUIDED POSITIVE SAMPLING TO INJECT PRIOR INTO SELF-SUPERVISED LEARNING

Aarash Feizi^{1,2}, Randall Balestriero³, Adriana Romero-Soriano^{1,2}, Reihaneh Rabbany^{1,2}

¹McGill University, ²Mila Institute, ³Independent
 {aarash.feizi, rrabba}@mail.mcgill.ca
 {randallbalestriero, adriana.romsor}@gmail.com

ABSTRACT

We propose *Guided Positive Sampling Self-Supervised Learning* (GPS-SSL), a general method to inject a priori knowledge into Self-Supervised Learning (SSL) positive samples selection. Current SSL methods leverage Data-Augmentations (DA) for generating positive samples and incorporate prior knowledge—an incorrect, or too weak DA will drastically reduce the quality of the learned representation. GPS-SSL proposes instead to design a metric space where Euclidean distances become a meaningful proxy for semantic relationship. In that space, it is now possible to generate positive samples from nearest neighbor sampling. Any prior knowledge can now be embedded into that metric space independently from the employed DA. From its simplicity, GPS-SSL is applicable to any SSL method, e.g. SimCLR or BYOL. A key benefit of GPS-SSL is in reducing the pressure in tailoring strong DAs. For example GPS-SSL reaches 85.58% on Cifar10 with weak DA while the baseline only reaches 37.51%. We therefore move a step forward towards the goal of making SSL less reliant on DA. We also show that even when using strong DAs, GPS-SSL outperforms the baselines on under-studied domains. We evaluate GPS-SSL along with multiple baseline SSL methods on numerous downstream datasets from different domains when the models use *strong* or *minimal* data augmentations. We hope that GPS-SSL will open new avenues in studying how to inject a priori knowledge into SSL in a principled manner.

1 INTRODUCTION

Self-supervised learning (SSL) has recently shown to be one of the most effective learning paradigm across many data domains (Radford et al., 2021; Girdhar et al., 2023; Assran et al., 2023; Chen et al., 2020; Grill et al., 2020; Bardes et al., 2021; Balestriero et al., 2023). SSL belongs to the broad category of annotation-free representation learning approaches, which have enabled machine learning models to use abundant and easy-to-collect unlabeled data, facilitating the training of ever-growing deep neural network architectures.

Despite the SSL promise, current approaches require handcrafted a priori knowledge to learn useful representations. This a priori knowledge is often injected through the positive sample—*i.e.*, semantically related samples—generation strategies employed by SSL methods (Chen et al., 2020). In fact, SSL representations are learned so that such positive samples get as similar as possible in embedding space, all while preventing a collapse of the representation to simply predicting a constant for all inputs. The different strategies to achieve that goal lead to different flavors of SSL methods (Chen et al., 2020; Grill et al., 2020; Bardes et al., 2021; Zbontar et al., 2021; Chen & He, 2021). In computer vision, positive sample generation mostly involves sampling an image from the dataset, and applying multiple handcrafted and heavily tuned data augmentations (DAs) to it, such as rotations and random crops, which preserve the main content of the image.

The importance of selecting the right DAs is enormous as it impacts performances to the point of producing a near random representation, in the worst case scenario (Balestriero et al., 2023). As such, tremendous time and resources have been devoted to designing optimal DA recipes, most notably for eponymous datasets such as ImageNet (Deng et al., 2009). From a practitioner’s

standpoint, positive sample generation could thus be considered solved if one were to deploy SSL methods *only* on such popular datasets. Unfortunately—and as we will thoroughly demonstrate throughout this paper—common DA recipes used in those settings fail to transfer to other datasets. For example, since ImageNet consists of natural images mostly focused around 1000 different object categories, we observe a reduction of performance on datasets consisting of more specialized images, such as hotel room images (Stylianou et al., 2019; Kamath et al., 2021), or only focused on different types of airplanes (Maji et al., 2013), or medical images (Yang et al., 2023). Since searching for the optimal DAs is computationally intense, there remains an important bottleneck when it comes to deploying SSL to new or under-studied datasets. This becomes particularly important when applying SSL methods on data gathered for real-world applications.

In this paper, we introduce a strategy to obtain positive samples, which generalizes the well established NNCLR SSL method (Dwibedi et al., 2021). While NNCLR proposes to obtain positive samples by leveraging known DAs and nearest neighbors in the embedding space of the network being trained, we propose to perform nearest neighbour search in an independently constructed embedding space. One special case could be to employ the embedding space of the network being trained—therefore recovering NNCLR—but more interestingly may also be generated by any pre-trained network, or even fully hand-crafted. This flexibility allows to (i) enable simple injection of prior knowledge into positive sampling without relying on tuning the DA, and most importantly (ii) makes the underlying SSL method much more robust to under-tuned DAs. By construction, the proposed method coined GPS-SSL for Guided Positive Sampling Self-Supervised Learning, can be coupled off-the-shelf with any SSL method used to learn representations, *e.g.*, BarlowTwins (Zbontar et al., 2021), SimCLR (Chen et al., 2020), BYOL (Grill et al., 2020). We validate the proposed GPS-SSL approach on a benchmark suite of under-studied datasets, namely FGVC Aircraft, PathMNIST, TissueMNIST, and show remarkable improvements over baseline SSL methods. We further evaluate our model on a real-world dataset, Revised-Hotel-ID (R-HID) (Feizi et al., 2022) and show clear improvements of our method compared the baseline SSL methods. Finally, we validate the approach on commonly used image datasets with known effective DAs recipes, and show that GPS remains competitive. Through comprehensive ablations, we show that GPS-SSL takes a step towards shifting the focus of designing *well-crafted DAs* to having a better *prior knowledge* embedding space in which choosing the nearest neighbour becomes an attractive positive sampling strategy.

The main contributions of this paper can be summarized as follows:

- We propose a positive sampling strategy, Guided Positive Sampling Self-Supervised Learning (GPS-SSL) that enables SSL models to use prior knowledge about the target-dataset to help with the learning process and reduce the reliance on carefully hand-crafted augmentations. The prior knowledge is an embedding space in which Euclidean based nearest neighbor sampling is informative of semantic relationship.
- We evaluate GPS-SSL by applying it to baseline SSL methods and show that with strong augmentations, they perform comparable to, or better than, the original methods. Moreover, they significantly outperform the original methods when using minimal augmentations, making it suitable for learning under-studied or real-world datasets (rather than transfer-learning).
- We further evaluate our model on datasets with under-studied applications, we consider hotel retrieval task in the counter human trafficking domain. Similar to benchmark datasets, we see on this less studied dataset, our proposed GPS-SSL outperforms the baseline SSL methods by a significant margin.

We provide the code for GPS-SSL and downloading and using R-HID on GitHub, available at: <https://github.com/aarashfeizi/gps-ssl>, for the research community.

2 RELATED WORK

Self Supervised Learning (SSL) is a particular form of unsupervised learning methods in which a given Deep Neural Network (DNN) learns meaningful representations of their inputs without labels.

The variants of SSL are numerous. At the broader scale, SSL defines a pretext task on the input data and train themselves by solving the defined task. In SSL for computer vision, the pretext tasks gener-

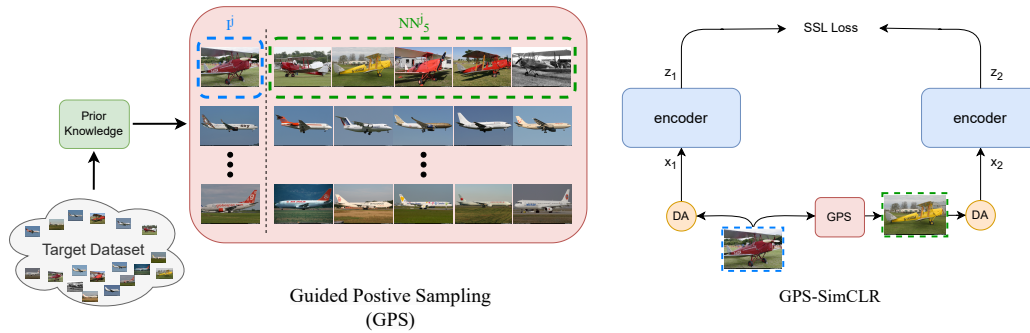


Figure 1: Our strategy, GPS-SSL, for positive sampling based on prior knowledge DA-based methods.

ally involve creating different views of images and encoding both so that their embeddings are close to each other. However, that criteria alone would not be sufficient to learning meaningful representations as a degenerate solution is for the DNN to simply collapse all samples to a single embedding vector. As such, one needs to introduce an “anti-collapse” term. Different types of solutions have been proposed for this issue, splitting SSL methods into multiple groups, three of which are: 1) Contrastive(Chen et al., 2020; Dwibedi et al., 2021; Kalantidis et al., 2020): this group of SSL methods prevent collapsing by considering all other images in a mini-batch as negative samples for the positive image pair and generally use the InfoNCE (Oord et al., 2018) loss function to push the negative embeddings away from the positive embeddings. 2) Distillation(Grill et al., 2020; He et al., 2020; Chen & He, 2021): these methods often have an asymmetric pair of encoders, one for each positive view, where one encoder (teacher) is the exponential moving average of the other encoder (student) and the loss only back-propagates through the student encoder. In general, this group prevents collapsing by creating asymmetry in the encoders and defines the pre-text task that the student encoder must predict the teach encoder’s output embedding. 3) Feature Decorrelation(Bardes et al., 2021; Zbontar et al., 2021): These methods focus on the statistics of the embedding features generated by the encoders and defines a loss function to encourage the embeddings to have certain statistical features. By doing so, they explicitly force the generated embeddings not to collapse. For example, Bardes et al. (2021) encourages the features in the embeddings to have high variance, while being invariant to the augmentations and also having a low covariance among different features in the embeddings. Besides these groups, there are multiple other techniques for preventing collapsing, such as clustering methods (Caron et al., 2020; Xie et al., 2016), gradient analysis methods (Tao et al., 2022).

Although the techniques used for preventing collapse may differ among these groups of methods, they generally require the data augmentations to be chosen and tuned carefully in order to achieve high predictive performance (Chen et al., 2020). Although choosing the optimal data augmentations and hyper-parameters may be considered a solved problem for popular datasets such as Cifar10 (Krizhevsky et al., 2009) or ImageNet (Deng et al., 2009), the SSL dependency on DA remains their main limitation to be applied to large real-world datasets that are not akin natural images. Due to the importance of DA upon the DNN’s representation quality, a few studies have attempted mitigation strategies. For example, Cabannes et al. (2023b) ties the impact of DA with the implicit prior of the DNN’s architecture, suggesting that informed architecture may reduce the need for well designed DA although no practical answer was provided. Cabannes et al. (2023a) proposed to remove the need for DA at the cost of requiring an oracle to sample the positive samples from the original training set. Although not practical, this study brings a path to train SSL without DA. Additionally, a key limitation with DA lies in the need to be implemented and fast to produce. In fact, the strong DA strategies required by SSL are one of the main computational time bottleneck of current training pipelines (Bordes et al., 2023). Lastly, the over-reliance on DA may have serious fairness implications since, albeit in a supervised setting, DA was shown to impact the DNN’s learned representation in favor of specific classes in the dataset (Balestriero et al., 2022).

All in all, SSL would greatly benefit from a principled strategy to embed a priori knowledge into generating positive pairs that does not rely on DA. We propose a first step towards such Guided Positive Sampling (GPS) below.

3 GUIDED POSITIVE SAMPLING FOR SELF-SUPERVISED LEARNING

We propose a novel strategy, *Guided Positive Sampling Self-Supervised Learning* (GPS-SSL), that obtains positive samples by nearest neighbor sampling from a designed embedding space and that greatly reduces the reliance of SSL on well-crafted DA to learning highly informative representations.

3.1 GPS-SSL: NEAREST NEIGHBOR POSITIVE SAMPLING IN A DESIGNED EMBEDDING SPACE

As theoretically shown in various studies (HaoChen et al., 2021; Balestriero & LeCun, 2022; Kiani et al., 2022), the principal factors that impacts the quality of the learned representation resides in how the positive pairs are defined. In fact, we recall that in all generality, SSL losses that are minimized can mostly be expressed as

$$\mathcal{L}_{\text{SSL}} = \sum_{(\mathbf{x}, \mathbf{x}') \in \text{PositivePairs}} \text{Distance}(f_{\theta}(\mathbf{x}), f_{\theta}(\mathbf{x}')) - \text{Diversity}(\{f_{\theta}(\mathbf{x}), \mathbf{x} \in \mathbb{X}\}), \quad (1)$$

for the mini-batch \mathbb{X} that gathers all the positive pair samples. A distance measure such as the ℓ_2 norm or the cosine similarity, and a diversity measure such that the rank of the embeddings or proxies of their entropy are used to match the positive pairs embedding all while preventing a representation collapse. All in all, defining the right set of PositivePairs is what determines the ability of the final representation to solve downstream tasks. The common solution is to repeatedly apply a DA onto a single datum to generate such positive pairs:

$$\text{PositivePairs} \triangleq \{(\text{DA}(\mathbf{x}), \text{DA}(\mathbf{x})), \forall \mathbf{x} \in \mathbb{X}\}, \quad (2)$$

where the DA operator includes the random realisation of the DA such as the amount of rotation or zoom being applied onto its input image. However, that strategy often reaches its limits since DAs need to be implemented for the specific data being used. When considering an image dataset, the challenge of designing DA for less common datasets, e.g., FGVC Aircraft, led practitioners to instead train the model on a dataset such as ImageNet, where strong DAs have already been discovered, and then transferring the model to other datasets. This however has its limits, e.g. when considering medical images.

As an alternative, we propose an off-the-shelf strategy to sample positive pairs that can be equipped onto any baseline SSL method, e.g., SimCLR, VICReg, coined GPS-SSL and which is defined by defining positive pairs through nearest neighbour sampling in a designed embedding space denoted as g_{γ} . First, let's define the collection of samples that are less than $\tau > 0$ away from a query sample $\mathbf{x} \in \mathbb{X}$ in the designed embedding space as

$$\mathcal{B}(\mathbf{x}) \triangleq \{\mathbf{x}' \in \mathbb{X} : \|g_{\gamma}(\mathbf{x}) - g_{\gamma}(\mathbf{x}')\|_2^2 < \tau\}. \quad (3)$$

From eq. (3), GPS-SSL simply obtains positive pairs by selecting the furthest point from \mathbf{x} in $\mathcal{B}(\mathbf{x})$ as in

$$\text{PositivePairs}_{\text{GPS}} \triangleq \{(\text{DA}(\mathbf{x}), \text{DA}(\mathbf{x}')), \forall (\mathbf{x}, \mathbf{x}') \in \mathbb{X}^2 : \mathbf{x}' = \arg \max_{\mathbf{u} \in \mathcal{B}(\mathbf{x})} \|g_{\gamma}(\mathbf{u}) - g_{\gamma}(\mathbf{x})\|_2^2\}, \quad (4)$$

We note that while we keep the DA operator in eq. (4), the quality of the learned representations will be shown to be much less sensitive to its design and strength compared to eq. (1). From this, we obtain a first direct result below making GPS-SSL recover a powerful existing method known as NNCLR.

Proposition 1 *For any employed DA, GPS-SSL which replaces eq. (2) by eq. (4) in any SSL loss (eq. (1)) recovers (i) input space nearest neighbor positive sampling when g_{γ} is the identity and $\tau \gg 0$, (ii) standard SSL when g_{γ} is a bijection and $\tau \rightarrow 0$, and (iii) NNCLR when $g_{\gamma} = f_{\theta}$ and $\tau \rightarrow 0$.*

The above result provides a first strong argument demonstrating how GPS-SSL does not reduce the capacity of SSL, in fact, it introduces a novel axis of freedom—namely the design of (g_{γ}, τ) —to extend current SSL beyond what is amenable solely by tweaking the original architecture f_{θ} , or the

original DA. In particular, the core motivation of the presented method is that this novel ability to design g_γ also reduces the burden to design DA. In fact, if we consider the case where the original DA is part of the original dataset

$$\forall \mathbf{x} \in \mathbb{X}, \exists \rho : \text{DA}_\rho(\mathbf{x}) \in \mathbb{X}, \quad (5)$$

so that for any sample in \mathbb{X} , there exists at least one DA configuration (ρ) that produces another sample, GPS-SSL can recover standard SSL albeit without employing any DA at all, as formalized below.

Theorem 1 *Performing standard SSL (employing eq. (2) into eq. (1)) with a given DA and a training set for which eq. (5) holds, is equivalent to performing GPS-SSL (employing eq. (4) into eq. (1)) without any DA and by setting g_γ to be invariant only to that DA, i.e. $g_\gamma(\text{DA}(\mathbf{x})) = g_\gamma(\mathbf{x})$.*

By construction from eq. (5) and assuming that one has the ability to design such an invariant g_γ , it is clear that the nearest neighbour within the training set for any $\mathbf{x} \in \mathbb{X}$ will be the corresponding samples $\text{DA}(\mathbf{x})$, therefore proving theorem 1. That result is quite impractical as designing such a mapping g_γ may prove as arduous as design its underlying DA, but nevertheless provides a great motivation to GPS-SSL. Namely, GPS-SSL does not limit SSL in any way and simply transfer the ability to embed a priori knowledge into SSL from a DA-only position to designing embedding spaces where Euclidean distances become semantically informative. Having the ability to design g_γ not only has the ability to encompass the burden of design a DA, and both can be used jointly.

The design of g_γ . The proposed strategy (eq. (4)) is based on finding the nearest neighbors of different candidate inputs in a given embedding space. There are multiple ways for acquiring an informative embedding space, i.e., a prescribed mapping g_γ . Throughout our study, we will focus on the most direct solution of employing a previously pretrained mapping. The pre-training may or may not have occurred on the same dataset being considered for SSL. Naturally, the alignment between both datasets affects the quality and reliability of the embeddings. If one does not have access to such pretrained model, another solution is to first learn an abstracted representation, e.g., an auto-encoder or VAE (Kingma & Welling, 2013), and then use the encoder for g_γ . In that setting the motivation lies in the final SSL representation being superior to solve downstream tasks than the encoder (g_γ) alone. We provide some examples of the resulting positive pairs with our strategy in Figure 1. In this figure, we use a pretrained model to calculate the set of k nearest neighbors for each image \mathbf{x} in the target dataset. Then for each image \mathbf{x} , the model randomly chooses the positive image from the nearest neighbors in embedding space (recall eq. (4)). Finally, both the original image and the produced positive sample are augmented using the chosen DA and passed as a positive pair of images through the encoders. Note that as per proposition 1, GPS-SSL may choose the image itself as its own positive sample, but the probability of it happening reduces as τ increases. As we will demonstrate the later sections, the proposed positive sampling strategy often outperforms the baseline DA based positive pair sampling strategy on multiple datasets.

Relation to NNCLR The commonality of NNCLR and GPS-SSL has been brought forward in proposition 1. In short, they both choose the nearest neighbor of input images as the positive sample. However, the embedding space in which the nearest neighbor is chosen is different; in NNCLR, the model being trained creates the embedding space which is thus updated at every training step, i.e., $g_\gamma = f_\theta$. However, GPS-SSL generalizes that in the sense that the nearest neighbors can stem from any prescribed mapping, without the constraint that it is trained as part of the SSL training, or even that it takes the form of a DNN. The fact that NNCLR only considers the model being trained to obtain its positive samples also makes it heavily dependent on complex and strong augmentations to produce non degenerate results. On the other hand, our ability to prescribe other mappings for the nearest neighbor search makes GPS-SSL much less tied to the employed DA. We summarize those methods in Figure 3.

3.2 EMPIRICAL VALIDATION ON BENCHMARKED DATASETS

In our experiments, we train the baseline SSL methods and the proposed GPS-SSL with two general sets of augmentations, *StrongAug*, which are augmentations that have been finetuned on the target dataset (for Cifar10 (Krizhevsky et al., 2009)) or ImageNet in the case of under-studied datasets (for FGVC Aircraft (Maji et al., 2013), PathMNIST (Yang et al., 2023), TissueMNIST (Yang et al.,

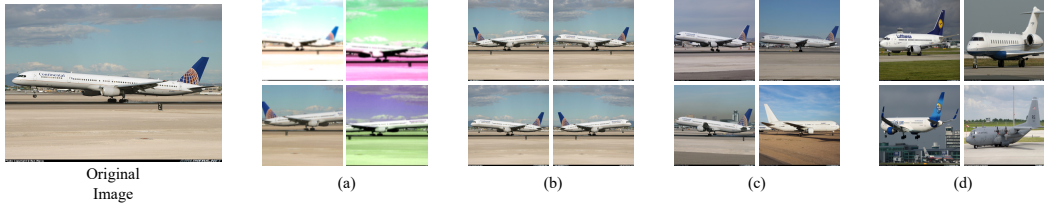


Figure 2: An example (a) *StrongAug* and (b) *RHFlipAug* applied to an image from the FGVCaircraft dataset. Furthermore, (c) and (d) depict examples of the 4 nearest neighbors calculated by CLIP and VAE embeddings, respectively.

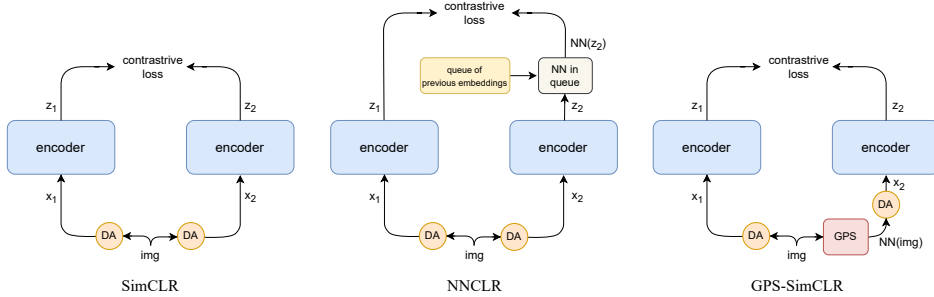


Figure 3: Architectures of SimCLR, NNCLR, and GPS-SimCLR. This figure demonstrates where the data augmentation (DA) happens in each method and also how the nearest neighbor (NN) search is different between NNCLR and GPS-SimCLR. Note that the ‘queue’ in NNCLR has a limited size, usually set to 65536. This issue could lead to under-represented classes to not be learned efficiently.

Table 1: Classification accuracy of a ResNet18 in different ablation settings; **Left:** Comparison GPS-SimCLR when different pretrained networks are used for generating embeddings for nearest-neighbor calculation, i.e., prior knowledge. **Right:** Best performance in *StrongAug* setting of SimCLR and GPS-SimCLR given different learning rates (LR).

GPS-SimCLR	FGVCaircraft		LR	FGVCaircraft	
	<i>RHFlipAug</i>	<i>StrongAug</i>		SimCLR	GPS-SimCLR
ViT-B _{MAE}	10.53	29.55	0.003	21.39	35.7
ViT-L _{MAE}	14.70	35.28	0.01	30.18	43.68
RN50 _{SUP}	18.15	41.47	0.03	39.27	49.57
RN50 _{VAE}	11.04	32.06	0.1	39.81	50.08
RN50 _{CLIP}	19.38	50.08	0.3	39.87	48.10

2023), and R-HID), and *RHFlipAug*, representing the scenario where we do not know the correct augmentations and use minimal ones. The set of *StrongAug* consists of random-resized-crop, random-horizontal-flip, color-jitter, gray-scale, gaussian-blur while solarization while *RHFlipAug* only uses random-horizontal-flip.

In order to thoroughly validate GPS-SSL as an all-purpose strategy for SSL, we consider SimCLR, BYOL, NNCLR, and VICReg as baseline SSL models, and for each of them, we will consider the standard SSL positive pair generation (eq. (2)) and the proposed one (eq. (4)). We opted for a *randomly-initialized* backbone ResNets (He et al., 2016) as the encoder. We also bring forward the fact that most SSL methods are generally trained on a large dataset for which strong DAs are known and well-tuned, such as Imagenet, and the learned representation is then transferred to solve tasks on smaller and less known datasets. In many cases, training those SSL models directly on those atypical dataset lead to catastrophic failures, as the optimal DAs have not yet been discovered. Lastly, we will consider five different embeddings for g_γ , one obtained from supervised learning, one from CLIP training (Radford et al., 2021) trained on LAION-400M Schuhmann et al. (2021), one for VAE (Kingma & Welling, 2013), and two for MAE (He et al., 2022) all trained on ImageNet and

Table 2: Classification accuracy of baseline SSL methods with and without GPS-SSL on four datasets on *ResNet50* using pretrained $RN50_{CLIP}$ embeddings for positive sampling. We consider both *StrongAug* (Strong Augmentation) and *RHFlipAug* (Weak Augmentation) settings. The set of DA used for *StrongAug* are random-resized-crop, random-horizontal-flip, color-jitter, gray-scale, gaussian-blur, and solarization. For the *RHFlipAug* setting, the only DA used is random horizontal flip. We mark the **first**, **second**, and **third** best performing models accordingly.

Aug.	Method	Datasets			
		Cifar10 (10 classes)	FGVCAircraft (100 classes)	PathMNIST (9 classes)	TissueMNIST (8 classes)
<i>RHFlipAug</i>	SimCLR	47.01	5.61	63.42	50.35
	BYOL	41.79	6.63	67.08	48.00
	NNCLR	28.46	6.33	56.70	37.98
	Barlow Twins	41.73	5.34	53.27	43.57
	VICReg	37.51	6.18	46.46	39.79
	GPS-SimCLR (ours)	85.08	18.18	87.79	53.14
	GPS-BYOL (ours)	84.07	13.50	87.67	53.05
	GPS-Barlow (ours)	84.45	17.34	88.77	56.63
	GPS-VICReg (ours)	85.58	18.81	88.91	56.44
<i>StrongAug</i>	SimCLR	90.24	47.11	93.64	58.53
	BYOL	90.50	34.23	93.29	56.63
	NNCLR	90.03	34.80	92.87	52.57
	Barlow Twins	88.34	18.12	92.03	61.69
	VICReg	91.21	38.74	93.22	60.18
	GPS-SimCLR (ours)	91.17	55.60	92.30	55.59
	GPS-BYOL (ours)	91.15	44.28	92.40	55.03
	GPS-Barlow (ours)	88.52	15.47	91.98	57.04
	GPS-VICReg (ours)	89.71	47.29	92.55	55.79

furthermore show our method is more robust to hyper-parameter changes (Table 1). Before delving in our empirical experiments, we emphasize that the supervised g_γ is employed in the *RHFlipAug* setting for two reasons. First, it provides what could be thought of as an optimal setting where the class invariants have been learned through the label information. Second, as a mean to demonstrate how one could combine a supervised dataset as a mean to produce prior information into training an SSL model on a different dataset. Since the said models are trained on ImageNet, all the provided results throughout this study remain practical since the labels of the target datasets, on which SSL models are trained and evaluated, are never observed for the training of neither g_γ nor f_θ .

Strong Augmentation Experiments. The DAs in the *StrongAug* configuration consist of strong augmentations that usually distort the size, resolution, and color characteristics of the original image. First, we note that in this setting, GPS-SSL generally does not harm the performance of the baseline SSL model on common datasets, i.e. Cifar10 (Table 2). In fact, GPS-SSL performs comparable to the best-performing baseline SSL model on Cifar10, i.e., VICReg, showcasing that GPS-SSL does not negatively impact performances even on those datasets. We believe that the main reason lies in the fact that the employed DA has been specifically designed for those datasets (and ImageNet). However, we observe that GPS-SSL outperforms (on FGVCAircraft and TissueMNIST) or is comparable to (on PathMNIST) the baseline SSL methods for the under-studied and real-world datasets. (Table 2). The reason for this is that, the optimal set and configuration of DA for one dataset is not necessarily the optimal set and configuration for another, and while SSL solely relies on DA for its positive samples, GPS-SSL is able to alleviate that dependency through g_γ and uses positive samples that can be more useful than default DAs, as seen in Figure 2. The results for these experiments can be seen in Table 2. Note that our method’s runtime is similar to the baseline SSL method on the dataset it is learning and does not hinder the training process (Figure 4).

Weak-Augmentation Experiments. We perform all experiments under the *RHFlipAug* setting as well, showing GPS-SSL produces high quality representations even in that setting, validating theorem 1. As seen in Table 2, GPS-SSL significantly outperforms all baseline SSL methods across both well-studied and under-studied datasets. These results show that our GPS-SSL strategy, though conceptually simple, coupled with the *RHFlipAug* setting, approximates strong augmentations used in the *StrongAug* configuration. This creates a significant advantage for GPS-SSL to be applied

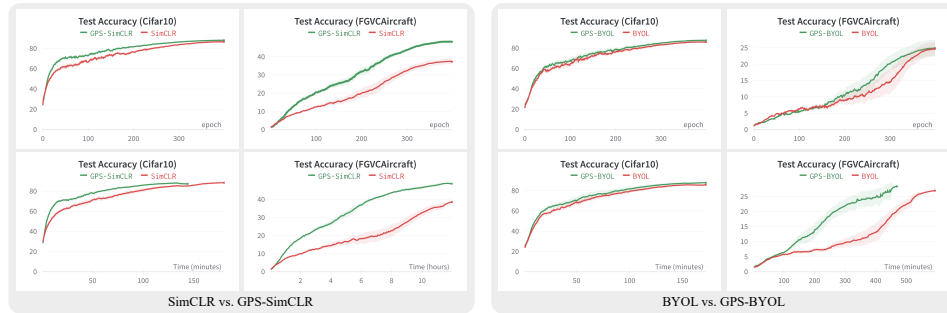


Figure 4: Comparing the runtime of BYOL vs. GPS-BYOL and SimCLR vs. GPS-SimCLR for two datasets, i.e., FGVCaircraft and Cifar10. In general, we see while the runtime of GPS-SSL remains the same as the original baseline SSL method, it improves the performance.

Table 3: Test accuracy comparison of GPS-SSL after 1K epochs versus 400 training epochs. We show the improvements of GPS-SimCLR are still significant on FGVCaircraft and comparable on Cifar10.

Method	Cifar10		FGVCaircraft	
	400 eps	1000 eps	400 eps	1000 eps
SimCLR	88.26	91.25	39.87	45.55
GPS-SimCLR	89.57	91.10	50.08	51.64
VICReg	89.34	90.61	33.21	41.19
GPS-VICReg	89.68	89.84	45.48	49.29

to real-world datasets where strong augmentations have not been found, but where the invariances learned by g_γ to generalize to them.

Ablation Study In this section we explore multiple ablation experiments in order to show GPS-SSL improves SSL and is indeed a future direction for improving SSL methods. First, we compare SSL and GPS training on Cifar10 and FGVCaircraft starting from a backbone initialized with random (realistic setting), supervised ImageNet pretrained, or CLIP pretrained weights to explore whether the improvement of GPS-SSL is due to better positive sampling or simply because of using a strong prior knowledge. We show in Table 4 that GPS-SSL performs better than the baseline SSL methods, even when they both have access to the pretrained network weights. This proves that the improvement in performance of GPS-SSL compared to baseline SSL methods is indeed due to better positive sampling.

Next, we compare GPS-SimCLR with three different embeddings for g_γ ; supervised, VAE, and CLIP embeddings. We observe that as the embeddings get higher in quality based on the pre-trained network, as the performance increases in both the *RHFlipAug* and *StrongAug* setting. However, note that even given the worst embeddings, i.e., the VAE embeddings, GPS-SimCLR still outperforms the original SimCLR in the *RHFlipAug* setting, showcasing that the nearest neighbors add value to the learning process when the augmentations are unknown.

We further explore if the improvement of GPS-SSL holds when methods are trained longer. To that end, we train a ResNet18 for 1000 epochs with SimCLR and VICReg with *StrongAug*, along with their GPS versions, on Cifar10 and FGVCaircraft and compare the results with the performance from 400 epochs. As seen in Table 3, the improvement of GPS-SSL compared to the baseline SSL method holds on FGVCaircraft dataset and remains comparable on Cifar10, showcasing the robustness of GPS-SSL.

Finally, we aim to measure the sensitivity of the performance of a baseline SSL method to a hyper-parameter, i.e., learning rate, with and without GPS-SSL. In this ablation experiment, we report the best performance of SimCLR and GPS-SimCLR given different learning rates in the *StrongAug* setting. We observe that GPS-SSL when applied to a baseline SSL method is as much, if not more, robust to hyper-parameter change. The results of both ablations are reported in Table 1. We further compare GPS-SSL with linear probing’s performance and other ablations in Appendix A.3.

4 CASE STUDY ON THE HOTELS IMAGE DATASET

In this section, we study how GPS-SSL compares to baseline SSL methods on an under-studied real-world dataset. We opt the R-HID dataset for our evaluation which gathers hotel images for the

Table 4: Comparing SimCLR with and without GPS-SimCLR with different initializations with a ResNet50. RAND, PT_{SUP} , and PT_{CLIP} represent random weights, ImageNet supervised weights, and CLIP pretrained weights.

Method	Weight Init.	Cifar10		FGVCAircraft	
		Weak Aug	Strong Aug	Weak Aug	Strong Aug
SimCLR	RAND	46.69	87.39	5.67	27.36
GPS-SimCLR		85.2	90.48	17.91	43.56
SimCLR	PT_{SUP}	43.99	94.02	17.91	59.92
GPS-SimCLR		91.3	95.53	39.45	66.88
SimCLR	PT_{CLIP}	45.57	90.26	6.21	41.04
GPS-SimCLR		89.44	91.23	24.15	49.63

purpose of countering human-trafficking. R-HID provides a single train set alongside 4 evaluation sets, each with a different level of difficulty.

Table 5: R@1 on different splits on R-HID Dataset for SSL methods. The splits are namely, \mathcal{D}_{SS} : {branch: seen, chain: seen}, \mathcal{D}_{SU} : {branch: unseen, chain: seen}, \mathcal{D}_{UU} : {branch: unseen, chain: unseen} and $\mathcal{D}_{??}$: {branch: unknown, chain: unknown}. We mark the best performing score in **bold**.

Method	\mathcal{D}_{SS}	\mathcal{D}_{SU}	\mathcal{D}_{UU}	$\mathcal{D}_{??}$
SimCLR	3.28	16.76	20.30	16.00
BYOL	3.69	19.27	23.02	18.47
Barlow Twins	3.04	15.54	18.96	15.06
VICReg	3.41	17.52	20.45	16.53
GPS-SimCLR (ours)	4.84	23.67	26.30	22.28
GPS-BYOL (ours)	3.89	19.64	23.18	19.38
GPS-Barlow (ours)	4.49	21.98	25.23	20.82
GPS-VICReg (ours)	5.33	25.71	28.29	23.78

We evaluate the baseline SSL models with and without GPS-SSL to the R-HID dataset and report the Recall@1 (R@1) for the different splits introduced. Based on the findings from 2, we adapt the *StrongAug* setting along with the prior knowledge generated by a CLIP-pretrained ResNet50.

As seen in Table 5, SSL baselines always get an improvement when used with GPS-SSL. The reason the baseline SSL methods underperform compared to their GPS-SSL version is that the positive samples generated only using DA lack enough diversity since the images from R-HID dataset have various features and merely DAs limits the information the network learns; however, paired with GPS-SSL, we see a clear boost in performance across all different splits due to the additional information added by the nearest neighbors.

5 CONCLUSIONS

In this paper we proposed GPS-SSL which presents a novel strategy to obtain positive samples for Self-Supervised Learning. In particular, GPS-SSL moves away from the usual DA-based positive sampling by instead producing positive samples from the nearest neighbors of the data as measure in some prescribed embedding space. That is, GPS-SSL introduces an entirely novel axis to research and improve SSL that is complementary to the design of DA and losses. Through that strategy, we were for example able to train SSL on atypical datasets such as medical images –without having to search and tune for the right DA. Those results open new avenues to the existing strategy of SSL pretraining on large dataset, and then transferring the model to those other datasets for which DAs as not available. In fact, we observe that while GPS-SSL meets or surpasses SSL performances across our experiments, the performance gap is more significant when the optimal DAs are not known, e.g., in PathMNIST and TissueMNIST we observe the performance of GPS-SSL with weak augmentations is slightly less than with strong augmentations. Besides practical applications, GPS-SSL finally provides a novel strategy to embed prior knowledge into SSL.

Limitations. The main limitation of our method is akin to the one of SSL, it requires the knowledge of the embedding in which the nearest neighbors are obtain to produce the positive samples. This limitation is on par with standard SSL’s reliance on DA, but its formulation is somewhat dual (recall theorem 1) in that one may know how to design such an embedding without knowing the appropriate DA for the dataset, and vice-versa. Alternative techniques like training separate and simple DNs to provide such embeddings prior to the SSL learning could be considered for future research.

REFERENCES

- Mahmoud Assran, Quentin Duval, Ishan Misra, Piotr Bojanowski, Pascal Vincent, Michael Rabbat, Yann LeCun, and Nicolas Ballas. Self-supervised learning from images with a joint-embedding predictive architecture. *arXiv preprint arXiv:2301.08243*, 2023.
- Randall Balestriero and Yann LeCun. Contrastive and non-contrastive self-supervised learning recover global and local spectral embedding methods. *Advances in Neural Information Processing Systems*, 35:26671–26685, 2022.
- Randall Balestriero, Leon Bottou, and Yann LeCun. The effects of regularization and data augmentation are class dependent. In S. Koyejo, S. Mohamed, A. Agarwal, D. Belgrave, K. Cho, and A. Oh (eds.), *Advances in Neural Information Processing Systems*, volume 35, pp. 37878–37891. Curran Associates, Inc., 2022. URL https://proceedings.neurips.cc/paper_files/paper/2022/file/f73c04538a5e1cad40ba5586b4b517d3-Paper-Conference.pdf.
- Randall Balestriero, Mark Ibrahim, Vlad Sobal, Ari Morcos, Shashank Shekhar, Tom Goldstein, Florian Bordes, Adrien Bardes, Gregoire Mialon, Yuandong Tian, et al. A cookbook of self-supervised learning. *arXiv preprint arXiv:2304.12210*, 2023.
- Adrien Bardes, Jean Ponce, and Yann LeCun. Vicreg: Variance-invariance-covariance regularization for self-supervised learning. *arXiv preprint arXiv:2105.04906*, 2021.
- Florian Bordes, Randall Balestriero, and Pascal Vincent. Towards democratizing joint-embedding self-supervised learning, 2023.
- Vivien Cabannes, Leon Bottou, Yann Lecun, and Randall Balestriero. Active self-supervised learning: A few low-cost relationships are all you need, 2023a.
- Vivien Cabannes, Bobak Kiani, Randall Balestriero, Yann Lecun, and Alberto Bietti. The SSL interplay: Augmentations, inductive bias, and generalization. In Andreas Krause, Emma Brunskill, Kyunghyun Cho, Barbara Engelhardt, Sivan Sabato, and Jonathan Scarlett (eds.), *Proceedings of the 40th International Conference on Machine Learning*, volume 202 of *Proceedings of Machine Learning Research*, pp. 3252–3298. PMLR, 23–29 Jul 2023b. URL <https://proceedings.mlr.press/v202/cabannes23a.html>.
- Mathilde Caron, Ishan Misra, Julien Mairal, Priya Goyal, Piotr Bojanowski, and Armand Joulin. Unsupervised learning of visual features by contrasting cluster assignments. *Advances in neural information processing systems*, 33:9912–9924, 2020.
- Ting Chen, Simon Kornblith, Mohammad Norouzi, and Geoffrey Hinton. A simple framework for contrastive learning of visual representations. In *International conference on machine learning*, pp. 1597–1607. PMLR, 2020.
- Xinlei Chen and Kaiming He. Exploring simple siamese representation learning. In *Proceedings of the IEEE/CVF conference on computer vision and pattern recognition*, pp. 15750–15758, 2021.
- Jia Deng, Wei Dong, Richard Socher, Li-Jia Li, Kai Li, and Li Fei-Fei. Imagenet: A large-scale hierarchical image database. In *2009 IEEE conference on computer vision and pattern recognition*, pp. 248–255. Ieee, 2009.
- Debidatta Dwibedi, Yusuf Aytar, Jonathan Tompson, Pierre Sermanet, and Andrew Zisserman. With a little help from my friends: Nearest-neighbor contrastive learning of visual representations. In *Proceedings of the IEEE/CVF International Conference on Computer Vision*, pp. 9588–9597, 2021.

-
- Arash Feizi, Arantxa Casanova, Adriana Romero-Soriano, and Reihaneh Rabbany. Revisiting hotels-50k and hotel-id. *arXiv preprint arXiv:2207.10200*, 2022.
- Rohit Girdhar, Alaaeldin El-Nouby, Zhuang Liu, Mannat Singh, Kalyan Vasudev Alwala, Armand Joulin, and Ishan Misra. Imagebind: One embedding space to bind them all. In *Proceedings of the IEEE/CVF Conference on Computer Vision and Pattern Recognition*, pp. 15180–15190, 2023.
- Jean-Bastien Grill, Florian Strub, Florent Alché, Corentin Tallec, Pierre Richemond, Elena Buchatskaya, Carl Doersch, Bernardo Avila Pires, Zhaohan Guo, Mohammad Gheshlaghi Azar, et al. Bootstrap your own latent-a new approach to self-supervised learning. *Advances in neural information processing systems*, 33:21271–21284, 2020.
- Jeff Z HaoChen, Colin Wei, Adrien Gaidon, and Tengyu Ma. Provable guarantees for self-supervised deep learning with spectral contrastive loss. *Advances in Neural Information Processing Systems*, 34:5000–5011, 2021.
- Kaiming He, Xiangyu Zhang, Shaoqing Ren, and Jian Sun. Deep residual learning for image recognition. In *Proceedings of the IEEE conference on computer vision and pattern recognition*, pp. 770–778, 2016.
- Kaiming He, Haoqi Fan, Yuxin Wu, Saining Xie, and Ross Girshick. Momentum contrast for unsupervised visual representation learning. In *Proceedings of the IEEE/CVF conference on computer vision and pattern recognition*, pp. 9729–9738, 2020.
- Kaiming He, Xinlei Chen, Saining Xie, Yanghao Li, Piotr Dollár, and Ross Girshick. Masked autoencoders are scalable vision learners. In *Proceedings of the IEEE/CVF conference on computer vision and pattern recognition*, pp. 16000–16009, 2022.
- Yannis Kalantidis, Mert Bulent Sariyildiz, Noe Pion, Philippe Weinzaepfel, and Diane Larlus. Hard negative mixing for contrastive learning. *Advances in Neural Information Processing Systems*, 33:21798–21809, 2020.
- Rashmi Kamath, Gregory Rolwes, Samuel Black, and Abby Stylianou. The 2021 hotel-id to combat human trafficking competition dataset. *arXiv preprint arXiv:2106.05746*, 2021.
- Bobak T Kiani, Randall Balestriero, Yubei Chen, Seth Lloyd, and Yann LeCun. Joint embedding self-supervised learning in the kernel regime. *arXiv preprint arXiv:2209.14884*, 2022.
- Diederik P Kingma and Max Welling. Auto-encoding variational bayes. *arXiv preprint arXiv:1312.6114*, 2013.
- Alex Krizhevsky, Geoffrey Hinton, et al. Learning multiple layers of features from tiny images. 2009.
- Subhransu Maji, Esa Rahtu, Juho Kannala, Matthew Blaschko, and Andrea Vedaldi. Fine-grained visual classification of aircraft. *arXiv preprint arXiv:1306.5151*, 2013.
- Aaron van den Oord, Yazhe Li, and Oriol Vinyals. Representation learning with contrastive predictive coding. *arXiv preprint arXiv:1807.03748*, 2018.
- Alec Radford, Jong Wook Kim, Chris Hallacy, Aditya Ramesh, Gabriel Goh, Sandhini Agarwal, Girish Sastry, Amanda Askell, Pamela Mishkin, Jack Clark, et al. Learning transferable visual models from natural language supervision. In *International conference on machine learning*, pp. 8748–8763. PMLR, 2021.
- Christoph Schuhmann, Richard Vencu, Romain Beaumont, Robert Kaczmarczyk, Clayton Mullis, Aarush Katta, Theo Coombes, Jenia Jitsev, and Aran Komatsuzaki. Laion-400m: Open dataset of clip-filtered 400 million image-text pairs. *arXiv preprint arXiv:2111.02114*, 2021.
- Abby Stylianou, Hong Xuan, Maya Shende, Jonathan Brandt, Richard Souvenir, and Robert Pless. Hotels-50k: A global hotel recognition dataset. *arXiv preprint arXiv:1901.11397*, 2019.

Chenxin Tao, Honghui Wang, Xizhou Zhu, Jiahua Dong, Shiji Song, Gao Huang, and Jifeng Dai. Exploring the equivalence of siamese self-supervised learning via a unified gradient framework. In *Proceedings of the IEEE/CVF Conference on Computer Vision and Pattern Recognition*, pp. 14431–14440, 2022.

Junyuan Xie, Ross Girshick, and Ali Farhadi. Unsupervised deep embedding for clustering analysis. In *International conference on machine learning*, pp. 478–487. PMLR, 2016.

Jiancheng Yang, Rui Shi, Donglai Wei, Zequan Liu, Lin Zhao, Bilian Ke, Hanspeter Pfister, and Bingbing Ni. Medmnist v2-a large-scale lightweight benchmark for 2d and 3d biomedical image classification. *Scientific Data*, 10(1):41, 2023.

Jure Zbontar, Li Jing, Ishan Misra, Yann LeCun, and Stéphane Deny. Barlow twins: Self-supervised learning via redundancy reduction. In *International Conference on Machine Learning*, pp. 12310–12320. PMLR, 2021.

A APPENDIX

A.1 R-HID SPLITTING METHOD

R-HID (Feizi et al., 2022) is created carefully to make sure no data leakage occurs. They mention how the total data is divided into the train and the multiple test splits. More specifically, first a set of chains (along with *all* their branches) are reserved for the \mathcal{D}_{UU} to make sure the chains (super-classes) and branches (classes) are not seen during training. Next, out of the remaining chains, a set of the branches are chosen to add *all* of their images to the \mathcal{D}_{SU} test split (since the training set will have other images from other branches from the same chain, but not the same branch images). Finally, out of the remaining branches, the images in each are split between \mathcal{D}_{SS} and train, creating the final test split that has a subset of the branches seen during training. With this procedure, they make sure of the table of overlapping below. More details regarding the splits is provided in the original paper.

A.2 HYPER-PARAMETER SEARCH

In all experiments, we train for 400 epochs with a batch size of 256 using one RTX 8000 GPU for all methods. To ensure we are choosing the correct hyper-parameters for a fair comparison, we search over a vast range of hyper-parameter combinations ($lr \in \{1e^{-3}, 3e^{-3}, 3e^{-2}, 1e^{-2}, 3e^{-1}, 1e^{-1}, 1\}$, $classifier_lr \in \{3e^{-2}, 1e^{-2}, 3e^{-1}, 1e^{-1}, 1, 3\}$, $weight_decay \in \{1e^{-4}, 1e^{-3}\}$) and for GPS-SSL with all SSL baselines we also search over $k \in \{1, 4, 9, 49\}$). For experiments using *RHFlipAug* and *StrongAug*, we use nearest neighbors calculated based on embeddings created from a ResNet50 that have been CLIP pre-trained as the prior knowledge. Finally, for each method, we report the best classification accuracy for Cifar10, FGVC Aircraft, PathMNIST, and TissueMNIST, and Recall@1 (R@1) for R-HID in Tables 2, 5, and 7. To calculate both metrics, we first train the encoder on the target dataset using the SSL method, with or without GPS-SSL. Then, for classification accuracy, we train a linear classifier on top of it, and for R@1, we encode all the images from the test set and calculate the percentage of images which their first nearest neighbor is from the same class.

A.3 ABLATION STUDY

A.3.1 DIFFERENT BACKBONE

First, we provide the same experiments as in Table 2, but trained with a ResNet18 instead of a ResNet50 and provide the results in Table 6. We see the same results for ResNet50 (discussed for Table 2) also hold when ran on a smaller architecture, i.e., ResNet18. This shows the improvements of GPS-SSL over baseline SSL methods is more reliable and robust.

A.3.2 FINETUNING FOR R-HID

We further try a trivial way of transferring knowledge from a pretrained network to other SSL baseline models and compare it to GPS-SimCLR; we initialize the base encoder in any SSL method, i.e.,

Table 6: Classification accuracy of baseline SSL methods with and without GPS-SSL on four datasets on *ResNet18* using pretrained $RN50_{CLIP}$ embeddings for positive sampling. We consider both *StrongAug* (Strong Augmentation) and *RHFlipAug* (Weak Augmentation) settings. The set of DA used for *StrongAug* are random-resized-crop, random-horizontal-flip, color-jitter, gray-scale, gaussian-blur, and solarization. For the *RHFlipAug* setting, the only DA used is random horizontal flip. We mark the **first**, **second**, and **third** best performing models accordingly.

Aug.	Method	Datasets			
		Cifar10 (10 classes)	FGVCAircraft (100 classes)	PathMNIST (9 classes)	TissueMNIST (8 classes)
<i>RHFlipAug</i>	SimCLR	47.62	7.70	62.99	52.30
	BYOL	49.72	8.99	77.77	51.00
	NNCLR	71.74	8.10	56.92	42.59
	Barlow Twins	42.00	7.53	64.82	49.43
	VICReg	36.04	4.95	56.92	50.26
	GPS-SimCLR (ours)	85.83	18.48	88.62	55.98
	GPS-BYOL (ours)	84.56	14.79	81.66	56.21
	GPS-Barlow (ours)	84.83	18.12	87.79	55.86
	GPS-VICReg (ours)	85.38	20.16	87.83	55.26
	<i>StrongAug</i>	SimCLR	88.26	39.87	91.56
BYOL		86.90	27.33	91.24	60.73
NNCLR		87.95	39.12	91.14	52.42
Barlow Twins		88.89	25.71	92.23	60.06
VICReg		89.34	33.21	92.27	59.41
GPS-SimCLR (ours)		89.57	50.08	92.19	62.76
GPS-BYOL (ours)		88.46	32.07	91.05	54.05
GPS-Barlow (ours)		88.39	25.35	91.55	62.93
GPS-VICReg (ours)		89.68	45.48	91.88	62.46

the ResNet18, to the pretrained network’s weights, as opposed to random initialization, and train it i.e., finetuning. Ultimately, we compare the results on R-HID in Table 7.

Although this might perform better if the pretrained network was trained on a visually similar dataset to the target dataset, Table 7 shows that it may harm the generalization on datasets that are different, e.g., ImageNet and R-HID, compared to being trained from scratch. However, GPS-SSL proves to be a stable method for transferring knowledge even if the pretrained and target dataset are visually different (Table 5).

A.3.3 COMPARING TO LINEAR PROBING

Finally, we compare the linear probing performance of the embeddings generated from different architectures, i.e. GPS backbones (GPS-BB), pretrained on different datasets, i.e., GPS Datasets (GPS-DS), with the performance of GPS-SSL using them. More specifically, in Tables 9 and 8, we compare the linear probe performance of the CLIP pretrained ResNet50 on LAION-400M (Schuhmann et al., 2021) along with vision transformers (ViTs) pretrained on ImageNet using Masked Auto Encoders (MAE) (He et al., 2022), a popular self-supervised method that also does not rely on strong augmentations. We see our method outperforms the linear probe accuracy of CLIP embeddings for both Cifar10 and FGVCAircraft and matches that of ViT-Base and ViT-Large for Cifar10 and ViT-Large for FGVCAircraft.

However, we further see that if we train the ViT-Large on the FGVCAircraft, using MAE with minimal augmentations, we can use that as the positive sampler for GPS-SSL and beat the baseline SSL method on FGVCAircraft. This shows that GPS-SSL does not entirely rely on huge pretrained mod-

Table 7: Comparing the R@1 performance of SSL methods on R-HID when trained from scratch against being initialized to a ImageNet pretrained network. The models with pretrained-initialized encoders (finetuned) are marked with ‘FT-’. We highlight the difference in R@1 of the pretrained against the scratch version with **green** when it improves and **red** when it worsens.

Method	\mathcal{D}_{SS}	\mathcal{D}_{SU}	\mathcal{D}_{UU}	$\mathcal{D}_{??}$
SimCLR	3.23	16.10	19.62	15.12
FT-SimCLR	-0.10	-0.21	-0.40	+0.27
BYOL	3.27	16.25	20.20	15.91
FT-BYOL	-0.57	-1.75	-2.23	-1.50
NNCLR	2.84	13.91	17.15	13.96
FT-NNCLR	-0.54	-2.44	-3.18	-2.67
VICReg	3.24	16.67	19.97	15.86
FT-VICReg	-0.43	-1.54	-2.45	-1.92

Table 8: Comparison of Linear probing (LP) and GPS-VICReg’s (with ResNet50) classification accuracy on FGVCaircraft with different GPS backbones (GPS BB) pretrained with CLIP and masked auto encoders (MAE) on different datasets without supervision (GPS DS). The performance of the vanilla VICReg is also depicted for comparison. RN50 and ViT-L refer to ResNet50 and ViT-Large, respectively.

GPS-BB	GPS-DS	LP	GPS-VICReg	VICReg
RN50 _{CLIP}	LAION-400M	44.55	46.44	39.99
ViT-L _{MAE}	ImageNet	37.32	38.44	
ViT-L _{MAE}	FGVCaircraft	17.01	42.87	

Table 9: Classification accuracy comparison of linear probing (LP) using embeddings with different GPS backbones (GPS-BB) pretrained with CLIP and masked auto encoders (MAE) on different upstream datasets, i.e. GPS-DS, and a trained ResNet50 with GPS-SimCLR on FGVCaircraft and Cifar10 using the same GPS backbones and datasets. RN50, ViT-L, and ViT-B refer to ResNet50, ViT-Large, and ViT-Base respectively.

GPS-BB	GPS-DS	Cifar10		FGVCaircraft	
		LP	GPS-SimCLR	LP	GPS-SimCLR
RN50 _{CLIP}	LAION-400M	87.85	91.17	44.55	53.81
ViT-B _{MAE}	ImageNet	85.78	87.35	27.96	29.55
ViT-L _{MAE}	ImageNet	91.45	90.11	37.29	35.28
ViT-L _{MAE}	FGVCaircraft	—	—	17.01	46.93

els and that there is potential possibilities for training a positive sampler prior to applying GPS-SSL to further boost the performance of baseline SSL methods.